Procedure of the turbulence wave number spectra reconstruction using the radial correlation reflectometry data

Gusakov E.Z., Kosolapova N.V., Heuraux S.*

Ioffe Institute, Politekhnicheskaya 26, 194021 St.Petersburg, Russia

**LPMIA, UMR-CNRS 7040, U H P, Nancy, France*

Fluctuation reflectometry is widely used technique providing information on the tokamak plasma micro turbulence. Technical simplicity and operation at a single access to plasma are among its merits, which however cause interpretation problems related to localization of measurements and wave number resolution. In order to improve the fluctuation reflectometry wave number selectivity a more sophisticated radial correlation reflectometry (RCR), using simultaneously different frequencies for probing was proposed and developed at numerous magnetic fusion devices. The coherence decay of two scattering signals with growing difference of probing frequencies is studied in this diagnostic and applied for estimation of the turbulence radial correlation length in a very straightforward manner. Namely, it is assumed that the distance between cut offs at which the correlation of two reflectometry signals is suppressed is equal to the turbulence correlation length.

However already in 1D numerical Born approximation analysis [1] a role of small angle scattering was shown, reducing the diagnostic spatial resolution and leading to a very slow decay of coherence in RCR. This effect was confirmed in RCR linear analytic theory in 1D and 2D model [2, 3], by 1D full-wave modeling [4] and 2D Born approximation computations [5] thus appealing for a more sophisticated RCR data interpretation.

In the present paper an analytical integral formula expressing the RCR cross-correlation function (CCF) in terms of turbulence radial wave number spectrum is analyzed and a procedure of its correct inversion for the spectrum determination from the CCF is proposed. The feasibility of this spectrum reconstruction procedure is confirmed in 1D numerical modeling performed both in linear approximation and using the full-wave approach. The method possibilities are studied in conditions relevant for experiments. The procedure accuracy dependence on probing frequency range and resolution as well as on the poor statistics and presence of noise is investigated.

The turbulence wave number spectrum reconstruction background

We treat the RCR problem using 1D model describing the O-mode probing by equation

$$\left\{\frac{d^2}{dx^2}+\frac{\omega^2}{c^2}-\frac{4\pi e^2\left[n(x)+\delta n(x)\right]}{m_e c^2}\right\}E_z(x,\omega)=0, \qquad (1)$$

where $n(x)=n_c(\omega_1)x/x_c(\omega_1)$ is the background density profile supposed linear in this paper and $\delta n(x)$ stands for turbulent fluctuations assumed statistically homogeneous. In the analytical section we suppose the transparent plasma size $x_c(\omega_1)$ and the turbulence correlation length l_c to be large enough to treat (1) in the WKB approximation. The corresponding solution takes a form of incident and reflected wave superposition

$$E=2E_0\left[1-\frac{n(x)+\delta n(x)}{n_c(\omega)}\right]^{-1/4}\exp\left[i\int_0^{x_c}\frac{\omega}{c}\sqrt{1-\frac{n(x)+\delta n(x)}{n_c(\omega)}}dx\right]\cos\left[\int_{x_c}^{x}\frac{\omega}{c}\sqrt{1-\frac{n(x')+\delta n(x')}{n_c(\omega)}}dx'+\frac{\pi}{4}\right] \qquad (2)$$

In the case the turbulence level is low enough, so that the reflected wave phase perturbations are small $\delta\varphi(\omega)=\frac{\omega}{c}\int_0^{x_c}\frac{\delta n(x)}{n_c(\omega)}\frac{dx}{\sqrt{1-n(x)/n_c(\omega)}}<1$, the fluctuation reflectometry signal is given by simple expression $\delta E=i\delta\varphi(\omega)E_0\exp\left[i\varphi_0(\omega)\right]$; $\left(\varphi_0(\omega)=2\int_0^{x_c}\frac{\omega}{c}\sqrt{1-\frac{n(x)}{n_c(\omega)}}dx\right)$.

Correspondingly, the RCR CCF is proportional to the phase perturbation correlation function, which may be expressed in terms of the turbulence wave number spectrum [2]. Finally the CCF takes a form

$$CCF=4\frac{\omega_1^2 x_c(\omega_1)}{c^2}\cdot\frac{\delta n^2}{n_c^2(\omega_1)}\int\frac{d\kappa}{2\pi}\frac{\tilde{n}_\kappa^2}{|\kappa|}e^{i\kappa\Delta}F\left[\sqrt{\kappa x_c(\omega_2)}\right]F^*\left[\sqrt{\kappa x_c(\omega_1)}\right]|E_0|^2\exp\left[i\left(\varphi_0(\omega_2)-\varphi_0(\omega_1)\right)\right] \qquad (3)$$

where $\Delta=x_c(\omega_1)-x_c(\omega_2)$ is the cut-off separation, δn^2 determines the density perturbation level, $F(s)=\int_0^s\exp\left(i\varsigma^2\right)d\varsigma$ is a Fresnel integral and the spectrum $\tilde{n}_\kappa^2$ is related to the density fluctuation correlation function by expression $2\pi\left\langle\delta n(x')\delta n(x'')\right\rangle=\delta n^2\int_{-\infty}^{\infty}\tilde{n}_\kappa^2\exp\left[i\kappa\left(x'-x''\right)\right]d\kappa$.

The $1/\kappa$ factor entering the integral in (3) is responsible for underlining the contribution of small angle scattering off long scale fluctuations into the RCR signal. This singularity saturated only for $\kappa x_c<1$ due to the Fresnel integral behavior ($F(s)\approx s$ at $s\ll 1$) leads to a very slow decrease of CCF mentioned above that complicates the RCR data interpretation. The way to exclude this singularity and reconstruct the turbulence wave number spectrum is provided by the similarity of (3) and Fourier transform. Namely, it is possible to show that the relation inverse to (3) expressing the turbulence spectrum in terms of CCF takes a form

$$\frac{\delta n^2}{n_c^2(\omega_2)}\tilde{n}_\kappa^2=\frac{\sqrt{i}}{2\sqrt{\pi}}\frac{c^2}{x_c(\omega_2)\omega_2^2}\frac{|\kappa|}{F\left[\sqrt{\kappa x_c(\omega_2)}\right]}\int CCF e^{-i\kappa\Delta}d\Delta \qquad (4)$$

where the CCF of the scattering (reflectometry) signals A_s obtained using the heterodyne detection is determined as

$$CCF = \frac{\left\langle \left[A_s(\omega_2) - \left\langle A_s(\omega_2) \right\rangle \right] \left[A_s^*(\omega_1) - \left\langle A_s^*(\omega_1) \right\rangle \right] \right\rangle}{\sqrt{\left\langle \left| A_s(\omega_2) - \left\langle A_s(\omega_2) \right\rangle \right|^2 \right\rangle \left\langle \left| A_s(\omega_1) - \left\langle A_s(\omega_1) \right\rangle \right|^2 \right\rangle}} \tag{5}$$

Numerical reconstruction of the turbulence spectrum and CCF

Here we shall analyze the accuracy of this inversion using the CCF computed numerically from (1) in the frame of full-wave modeling or Born approximation (the scattering signal in this case is given by expression $A_s = \frac{i\omega\sqrt{S_i}}{16\pi}\int_0^\infty \frac{\delta n(x)}{n_c} E_0^2(x)dx$ where electric field $E_0(x)$ is normalized to unite power flux density). In the later case the superposition of $m=10^4$ harmonics $\delta n(x) = \delta n_0 \sum_{j=1}^{j=m} \cos(jqx + \varphi_j)\sqrt{\frac{2q}{\pi}\tilde{n}_{jq}^2}$ possessing wave numbers jq, random phases φ_j, and amplitude distributed in accordance with the turbulence spectrum $\tilde{n}_\kappa^2$ is used in analysis. The calculation parameters are as follows: $x_c = 40cm$; correlation length $l_c = 2cm$; $\omega_1 = 6\cdot 10^{11} c^{-1}$ The averaging is performed over ensemble of typically 500 random phase samples. In the case of spectrum $\tilde{n}_\kappa^2 = \sqrt{\pi} l_c e^{-l_c^2\kappa^2/4}$, shown in fig. 1a by red curve, the CCF calculated in the interval $-20l_c < \Delta < 20l_c$ is shown in fig. 1b by the black curve. It is much broader than turbulence Gaussian correlation function (red curve in fig. 1b), asymmetric and possesses small, but finite imaginary part, shown by green line. As it is obvious, the CCF provides no information on the turbulence correlation function. Accordingly, the CCF spectrum obtained after extrapolation of the CCF to higher Δ values is very peaked around the zero wave number, unlike the initial Gaussian spectrum. However after been treated in agreement with (4) its real part takes a form similar to the Gaussian (see black curve in fig. 1a). The oscillations of the reconstructed real part of the spectrum around the Gaussian one are produced by discontinuities of the extrapolation procedure at $\Delta = \pm 20l_c$. A smaller imaginary part of the

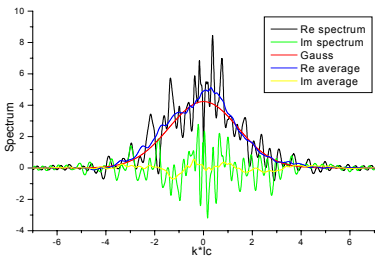

Fig. 1a. The spectrum versus normalized wave number.

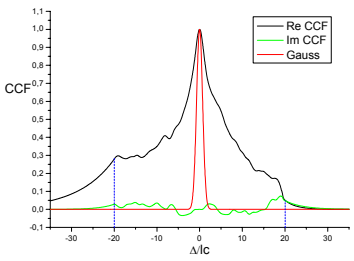

Fig. 1b. The signal and turbulence CCF.

reconstructed spectrum (shown by green line in fig. 1a) is oscillating around the zero line. Smoothing of these oscillations by integrating over a wave number interval results in a spectrum similar to Gaussian and possessing very small imaginary part, as it is shown in fig. 1a by blue and yellow lines, correspondingly. It is important to note that these oscillations originated by extrapolation procedure could be removed to the matching region $\Delta = \pm 20 l_c$ by performing Fourier transform of the reconstructed spectrum providing the turbulence CCF. The result of this transformation in the case of spectrum of fig. 1a is shown in fig. 2a. As it is seen there, the reconstructed real part of the turbulence CCF fits perfectly the initial Gaussian correlator at $\Delta < 2l_c$. The finite value of the CCF imaginary part, as well as CCF random behavior at $\Delta > 2l_c$ should be attributed to imperfect averaging. As it is seen in fig. 2b, the level of the reconstructed CCF imaginary part as well as its real part at $\Delta > 2l_c$ is suppressed by increasing the averaging ensemble from 500 to 1000 and then to 10000 samples. Using the approach based on relation (4) we have also reconstructed a multi component spectrum shown in fig. 3a by red curve. The corresponding turbulence CCF shown in fig. 3b by red curve possesses a typical oscillatory structure. The RCR CCF real part shown there by the blue curve is very different from the original one, however application of the reconstruction procedure based on (4) results in complex spectrum, real part of which fits well the original turbulence spectrum even without smoothing (black line in Fig.3a), whereas the imaginary one (green line in Fig.3a) oscillates around zero and is removed by smoothing. The Fourier transform of the obtained spectrum results in the perfect turbulence CCF reconstruction, shown in fig. 3b by the black curve.

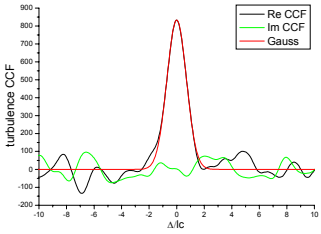

Fig. 2a. The turbulence CCF.

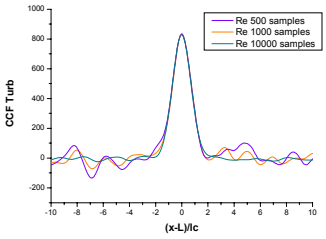

Fig. 2b. The turbulence CCF.

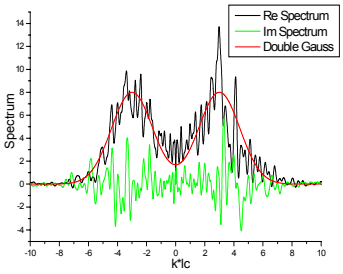

Fig. 3a. The turbulence spectrum.

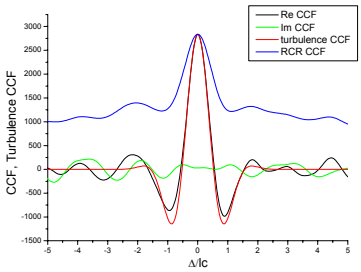

Fig. 3b. The turbulence CCF.

In the case of exponential spectrum $\tilde{n}_\kappa^2 = 0.5 l_c e^{-|\kappa| l_c}$, suppressed at small wave numbers, shown in fig. 4a by red curve, the CCF calculated in the interval $-20 l_c < \Delta < 20 l_c$ is shown in fig. 4b by the blue curve. It is much broader than turbulence Gaussian correlation function (red curve in fig. 4b), asymmetric and possesses small, but finite imaginary part, shown by green line. Accordingly, the CCF spectrum obtained after extrapolation of the CCF to higher Δ values is very peaked around the zero wave number, unlike the initial spectrum. However after been treated in agreement with (4) its real part takes a form similar to the turbulence spectrum (see black curve fig. 4a). The oscillations of the reconstructed real part of the spectrum around the initial one are produced by discontinuities of the extrapolation procedure at $\Delta = \pm 20 l_c$. A smaller imaginary part of the reconstructed spectrum (shown by green line in fig. 1a) is oscillating around the zero line.

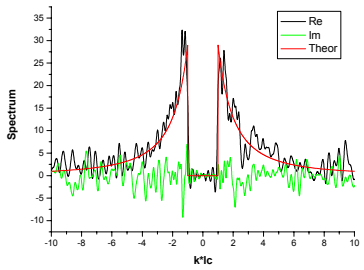

Fig. 4a. The reconstructed spectrum versus normalized wave number.

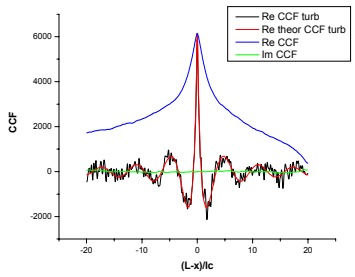

Fig. 4b. The signal and reconstructed turbulence CCF.

It is important to note that these oscillations originated by extrapolation procedure could be removed to the matching region ($\Delta = \pm 20 l_c$ in the present computation) by performing Fourier transform of the reconstructed spectrum providing the turbulence CCF. The result of this transformation in the case of spectrum of fig. 1a is shown by black curve in fig. 1b. As it is seen there, the reconstructed real part of the turbulence CCF fits perfectly the initial turbulence CCF describing not only the kernel of the CCF at $\Delta < 2 l_c$, but also oscillations caused by the spectrum discontinuity. In Fig. 4 we have performed reconstruction based on the signal CCF computed in a very wide signal frequency range corresponding to $|\Delta| \le 20 l_c$ not possible in the experiment. In Fig. 5 the reconstructed Gaussian turbulence

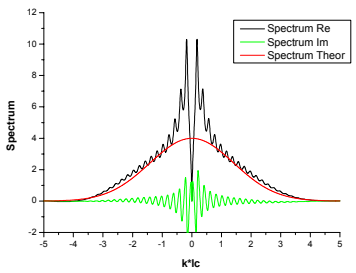

Fig. 5a. The reconstructed turbulence spectrum.

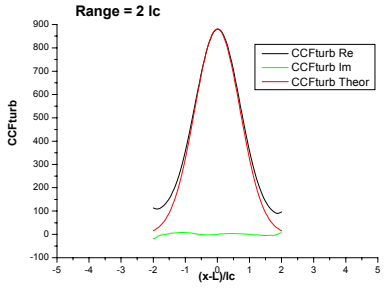

Fig. 5b. The reconstructed turbulence CCF.

spectra and CCF are shown for the realistic case $|\Delta| \le 2l_c$. As it is seen there, in spite of the fact the reconstructed spectrum (black curve) is different from the initial Gaussian spectrum (red curve) the obtained turbulence CCF fits the Gaussian well. The previous evaluation of the CCF used for the reconstruction in Fig.4 was performed with fine spatial resolution in a wide region (10000 points in the $[-20l_c, 20l_c]$ interval), which corresponds to probing with

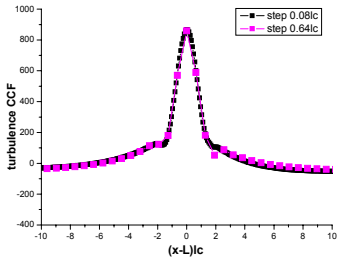

Fig. 6. The turbulence CCF reconstructed at $|\Delta| \le 2l_c$ and $|\delta\Delta| = 0.08l_c$ and $|\delta\Delta| = 0.64l_c$.

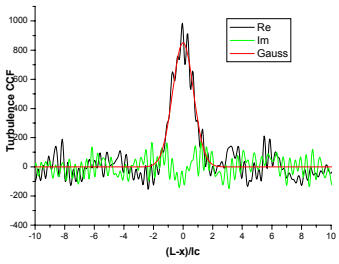

Fig. 7a. The turbulence CCF reconstruction at 10% SNR, 500 samples.

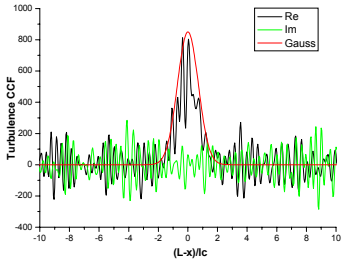

Fig. 7b. The turbulence CCF reconstruction at 100% SNR, 10000 samples.

the very detailed frequency resolution and in a very wide range not always possible in the experiment. In more realistic conditions of only 6 RCR measurements the reconstruction of the turbulence CCF is also possible, as we show in Fig.6 based on the RCR data obtained at $|\Delta| < 2l_c$ with the signal frequency cut off step $|\delta\Delta| = 0.08l_c$ and $|\delta\Delta| = 0.64l_c$.

Very important for the feasibility of the proposed procedure is its weak sensitivity to the experimental noise. As it is seen in Fig.7a and 7b, in the case of 10% SNR the reconstruction of the Gaussian turbulence CCF is possible with averaging performed over only 500 random turbulence samples, whereas in the case of 100% SNR 10000 samples are needed.

The application of the developed procedure to the full-wave modeling of (1) using the numerical scheme described in [4] and following parameters: $x_c = 20cm$; $l_c = 0.25cm$; $\omega_1 = 1.9 \cdot 10^{11} c^{-1}$ also resulted in successful reconstruction of rectangular turbulence spectrum in spite of correlation length been smaller than the probing wavelength, as it is seen in fig. 8.

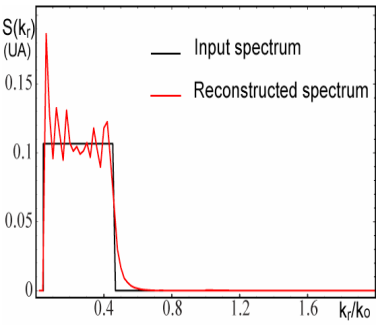

Fig. 8. The turbulence spectrum.

Conclusion

Concluding it is worth to underline that application of the proposed procedure to the turbulence spectrum and CCF reconstruction from the RCR data in numerical modeling have

led to very promising results in conditions relevant for experiments. The demonstrated possibility of fine reconstruction, at least in 1D geometry, is proving the procedure feasibility and appealing for further optimization and tests in 2D numerical modeling.

Acknowledgements

Financial support by RFBR (grants 09-02-00453, 07-02-92162-CNRS), NWO-RFBR Centre of Excellence on Fusion Physics and Technology (grant 047.018.002), ANR_blanc_06_0084, scientific school grant-1550.2008.2 and by Dynasty Foundation is acknowledged.

References

[1] Hutchinson I 1992 Plasma Phys. Control. Fusion 34 1225
[2] Gusakov E Z and Popov A Yu 2002 Plasma Phys. Control. Fusion 44 2327
[3] Gusakov E Z and Yakovlev B O 2002 Plasma Phys. Control. Fusion 44 2525
[4] G Leclert, S Heuraux, E Z Gusakov et al. 2006 Plasma Phys. Control. Fusion 48 1389–1400
[5] Gusakov E Z, et al. 34th EPS Conf. on Plasma Phys. Warsaw, 2 - 6 July 2007 ECA Vol.**31F**, P-5.100 (2007)